ELSEVIER

Physica D 88 (1995) 176–186

PHYSICA D

Strange non-chaotic attractor in a quasiperiodically forced circle map

Ulrike Feudel, Jürgen Kurths, Arkady S. Pikovsky

Max-Planck-Arbeitsgruppe "Nichtlineare Dynamik", Universität Potsdam, Potsdam, Germany

Received 20 January 1995; revised 31 May 1995; accepted 31 May 1995
Communicated by F.H. Busse

Abstract

We show that in the quasiperiodically forced circle map strange non-chaotic attractors can appear for non-linearities far from the border of chaos. The destruction of a two-frequency quasiperiodic torus connected with the appearance of a strange non-chaotic attractor is described in detail. This strange non-chaotic attractor is characterized by logarithmically slow diffusion of the phase. It is shown that in this regime the high-order phase-locking states disappear and the rotation number varies rather smoothly with the parameters.

1. Introduction

Strange non-chaotic attractors (SNA) typically appear in quasiperiodically forced non-linear dynamical systems. These attractors were firstly described by Grebogi et al. in 1984 [1] and since then investigated in a number of numerical [2–12] and experimental [13,14] studies. A typical system considered in most of these works is a non-linear continuous- or discrete-time oscillator with a quasiperiodic two-frequency forcing. Strange non-chaotic attractors, which are observed in such a system, exhibit some properties of regular as well as chaotic systems. Like regular attractors they have only negative and zero (connected to the quasiperiodic forcing) Lyapunov exponents; like usual chaotic attractors they are fractals. Also, their correlation properties lie in between order and chaos: as shown in [11], they can have a singular continuous spectrum.

In this paper we investigate a SNA in the quasiperiodically forced circle map. The circle map is one of the simplest models of non-linear dynamics, and, fortunately, is also highly relevant for understanding of many physical phenomena (see, e.g., [15]). For example, with the circle map one can describe the phase-locking structure (devil's staircase) of a periodically forced non-linear oscillator. Furthermore, the voltage–current characteristics of a driven Josephson junction can be related to the circle map [16]. Here we focus on the properties of the quasiperiodically forced circle map, which is relevant for understanding of the dynamics of a non-linear oscillator, forced with two incommensurate frequencies. With the circle map one can describe both regular oscillations and the transition to chaos. Here we do not consider chaotic regimes, nevertheless, rather complex dynamical regimes with SNA are shown to exist even far away from the transition to chaos.

The paper is organized as follows. In Section 2 we describe the basic properties of the circle map. We

SSDI 0167-2789(95)00205-7

also review here previous works on the quasiperiodically forced circle map. In Section 3 the methods of characterization of strange non-chaotic attractors are discussed. These methods are applied to the quasiperiodically forced circle map in Section 4. We show that SNA can exist in certain parameter ranges which are far from the chaotic region and which correspond to the Arnol'd tongue with zero rotation number in the unforced map. Furthermore, we discuss the dependence of the width of the Arnol'd tongue on the forcing to study the influence of the forcing on the form of the devil's staircase.

2. Basic model

We investigate the following model:

$$x(t+1) = x(t) + B + \frac{A}{2\pi}\sin[2\pi x(t)] + \varepsilon \sin[2\pi\theta(t)], \quad (1)$$

$$\theta(t+1) = \theta(t) + \omega \mod 1, \quad (2)$$

where B, A, and ε are parameters and ω is irrational. Because the r.h.s. of (1) is periodic in x with period 1, one can consider x as a phase variable and Eq. (1) as the quasiperiodically forced circle map. Quasiperiodicity means the presence of at least two incommensurate frequencies; here these are 1 (due to discreteness of time) and ω. The parameter ε represents the amplitude of the force, while the parameters B and A govern phase shift and non-linearity in the circle map.

2.1. The circle map and its properties

We first review well-known properties of the circle map (see, e.g., [17,15]) and describe previous results on the system (1), (2). If the amplitude of the force ε vanishes, Eq. (1) describes the circle map. For small non-linearity $A < 1$, this map is invertible and has no chaotic trajectories. The dynamics of the map can be characterized by the rotation number defined as

$$\rho = \lim_{t\to\infty} \frac{x(t) - x(0)}{t}. \quad (3)$$

This rotation number can be either rational or irrational. If $\rho = p/q$ with integers p and q, the circle map has a stable and an unstable periodic orbit satisfying $x(t+q) = x(t) + p$. To each of such phase-locked regime corresponds a region in the plane of parameters A, B—the so-called Arnol'd tongue. Between these tongues the rotation number is irrational. In the circle map tongues with all rationals exist and are everywhere dense, however the measure of parameter values corresponding to the two-frequency quasiperiodic motion is non-zero. For a fixed non-linearity $A = \text{const.} < 1$, the dependence of ρ on B is a monotonous continuous function, having constant values inside all tongues—the so-called devil's staircase. The transition from a phase-locked regime to a quasiperiodic one as the parameter B changes occurs via the tangent bifurcation at which the stable and unstable periodic orbits collide; at the bifurcation point the marginally stable periodic orbit with zero Lyapunov exponent exists. The quasiperiodic motion is also characterized by zero Lyapunov exponent.

2.2. Quasiperiodically forced circle map: a review of previous results

In the quasiperiodically forced circle map (1), (2) the dynamics of θ is added to the dynamics of x. Thus, even in the decoupled case $\varepsilon = 0$, the additional frequency ω is added to the regimes of the circle map: a stable (unstable) periodic orbit becomes a stable (unstable) two-frequency quasiperiodic motion, and a quasiperiodic motion becomes a three-frequency quasiperiodic motion. On the phase plane (x, θ) the two-frequency quasiperiodic motion is represented by an invariant curve (see Fig. 1). This curve can be regarded as a cross-section (Poincaré map) of a two-frequency torus in a three-dimensional phase space of a continuous-time dynamical system. Thus, we use the term "two-frequency torus" to describe this invariant curve. Similarly, we say that a three-frequency motion is represented by a three-frequency torus.

A detailed numerical study of system (1), (2) for $\varepsilon \neq 0$ has been performed in Refs. [2–5,12]. It has been found that for $\varepsilon \neq 0$ on the plane of parameters A, B three regions exist, characterized by the existence of three-frequency torus, strange non-chaotic attractor, and chaotic attractor, respectively

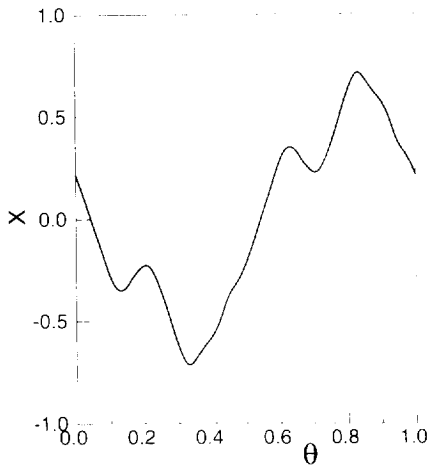

Fig. 1. Phase portrait of the two-frequency torus in system (1),(2) for $A = 0.8$, $B = 0$, and $\varepsilon = 1.1$. 15000 iterations forming an invariant curve are plotted.

(two-frequency torus exists in all regions). It has also been suggested that one can distinguish between the different regimes by means of the Lyapunov exponent (the Lyapunov exponent corresponding to the variable θ in (2) is always zero, only the non-trivial Lyapunov exponent which corresponds to the variable x is considered in [2–5,12] and throughout this paper) and the rotation number (3). The two-frequency torus and the strange non-chaotic attractor are characterized by negative Lyapunov exponent, and the three-frequency torus by zero Lyapunov exponent. In [2–5,12] it was suggested that the two-frequency torus has a rotation number satisfying the resonance condition

$$\rho = \frac{p + l\omega}{q} \tag{4}$$

(p, l, and q are integers), whereas for SNAs and the three-frequency tori $\rho \neq (p + l\omega)/q$. It was also argued that the dependence of ρ on B for fixed ε and A demonstrates a complete devil's staircase with all resonances of type (4) being present.

Another approach to study the quasiperiodically circle map (1), (2) has been recently suggested in Ref. [18]. There a method of finding a border of a two-frequency tongue on a plane of parameters has been proposed, and it has been shown that for relatively small values of non-linearity A and external force amplitude ε the bifurcation of collision of a stable and unstable two-frequency tori is similar to a tangent bifurcation in the circle map.

In our previous paper [9] we proposed methods to distinguish between strange and non-strange non-chaotic attractors. Now we apply these techniques to characterize different regimes in the quasiperiodically forced circle map. For small external force our results agree with the findings of [18]. We investigate in detail a transition to a strange non-chaotic attractor and show that the conjectures of Refs. [2–5,12] concerning the classification of attractors according to the rotation number are not valid for the region of parameters we study. We demonstrate also that the appearance of the strange non-chaotic attractor leads to destruction of the devil's staircase.

3. Methods of investigation

In this section we briefly review the techniques of characterizing strange non-chaotic attractors, described in Ref. [9]. We treat general dynamical systems of the form

$$x(t+1) = f[x(t), \theta(t)], \tag{5}$$

$$\theta(t+1) = \theta(t) + \omega \mod 1, \tag{6}$$

where $f(x, \theta)$ is periodic in θ with period 1 and ω is irrational.

3.1. Rational approximations

Let us approximate the irrational ω in (6) with rationals $\omega_n = p_n/q_n$,where p_n and q_n can be in the usual way obtained from the continued fraction representation of ω [19,20]. Then (6) produces a periodic orbit $(\theta_0, \theta_0 + \omega_n, \ldots, \theta_0 + (q_n - 1)\omega_n)$ of period q_n and (5) is a periodically forced map. This map can have an attractor, which generally depends on the initial phase θ_0. A combination of all attractors for different θ_0 gives an approximation to the attractor in the quasiperiodically forced system. To distinguish between strange and non-strange (smooth) attractors we construct a bifurcation diagram using this initial phase θ_0 as a bifurcation parameter. The form of these

bifurcation diagrams yields one criterion to characterize the structure of the attractor: If in the rational approximations with arbitrary large p_n and q_n one observes bifurcations of the attractors as the parameter θ_0 is varied, then the quasiperiodically forced system possesses a strange non-chaotic attractor. If there are no bifurcations then the attractor is smooth. The possibility for the attractor to be chaotic is excluded by the additional condition that the Lyapunov exponent be negative. For the system considered in Ref. [9] the period-doubling and the pitchfork bifurcation are observed. For the circle map with $A < 1$, which is one-to-one, one can expect only tangent and pitchfork bifurcations, where stable and unstable periodic orbits with the same period are created (annihilated), to occur.

3.2. Phase sensitivity and local Lyapunov exponents

As mentioned above, a strange non-chaotic attractor has negative Lyapunov exponent, so there is no sensitive dependence on initial conditions. However, as was shown in Ref. [9], such attractors demonstrate sensitive dependence with respect to the external phase θ. Quantitatively, this sensitivity is measured by the phase sensitivity exponent, which is defined as follows. Simultaneously with iterations of (5), (6), one can iterate the "phase derivative" x_θ:

$$x_\theta(t+1) = f_x[x(t),\theta(t)]x_\theta(t) + f_\theta[x(t),\theta(t)]. \tag{7}$$

These iterations depend on the initial point $x(0),\theta(0)$ on the attractor, and the attractor as a whole can be characterized with the phase sensitivity function

$$\Gamma(T) = \min_{x(0),\theta(0)}\left[\max_{1\le t\le T} x_\theta(t)\right]. \tag{8}$$

For non-strange attractors this function $\Gamma(T)$ saturates for large T giving the largest possible value of the derivative x_θ, while for strange non-chaotic attractor it grows unbounded, typically as

$$\Gamma(T) \sim T^\mu, \tag{9}$$

where μ is called the phase sensitivity exponent. In [9] it was also discussed how to obtain the phase sensitivity properties from a time series.

This phase sensitivity is caused by the existence of positive local Lyapunov exponents (for the concept of local Lyapunov exponents see, e.g., [21,22]). This means that although in average there is no sensitivity to initial conditions, on the attractor there are regions where this sensitivity is present, and it is responsible for the phase sensitivity property. The local (corresponding to finite time T) Lyapunov exponent is defined as

$$\Lambda_T = \frac{1}{T}\sum_{t=1}^{T} \log|f_x[x(t),\theta(t)]|.$$

For large T the distribution function of local Lyapunov exponents scales as

$$\mathrm{prob}(\Lambda_T = \Lambda) \sim \exp(-T\phi(\Lambda))$$

with a scaling function ϕ [22]. The existence of positive local Lyapunov exponents means that $\phi(\Lambda) > 0$ for some interval of values of $\Lambda > 0$. This allows arbitrary large local expansion rates $\prod_1^T |f_x|$ to be observed, and therefore the phase sensitivity function (8) is unbounded.

4. Results for the quasiperiodically forced circle map

In this section we apply the methods described above to characterize the attractors and their transitions in the quasiperiodically forced circle map (1), (2). We fix the frequency ω to be the reciprocal of the golden mean: $\omega = (\sqrt{5}-1)/2$. The rational approximation of this frequency are given by the ratios of Fibonacci numbers $\omega_n = F_{n-1}/F_n$, where $F_1 = F_2 = 1$, $F_{n+1} = F_n + F_{n-1}$. Also, in this paper we fix the parameter of non-linearity $A = 0.8$. This value is less than 1, so we exclude the possibility of chaotic behavior in the system (1), (2). The main parameters varied are the amplitude of the quasiperiodic force ε and the phase shift B. We especially restrict our attention to a region of small (in absolute value)

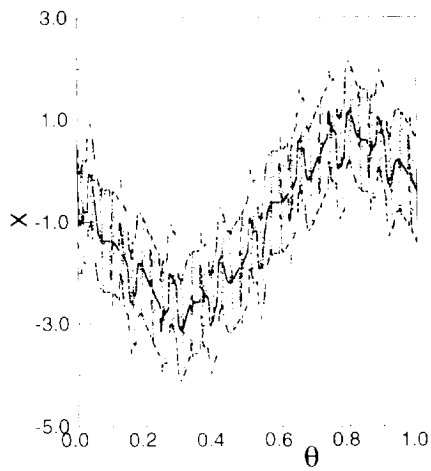

Fig. 2. The same as Fig. 1, but in the regime with the SNA for $\varepsilon = 3.1$.

values of B, i.e. we will investigate what happens inside the widest Arnol'd tongue, corresponding to the zero rotation number of the autonomous circle map.

4.1. Destruction of the smooth torus

Consider first the case $B = 0$. For relatively small amplitudes of the external force ε a two-frequency torus is observed in the system (1), (2), see Fig. 1. Approximately at $\varepsilon = \varepsilon_c^1 \approx 2.991$ the torus is destroyed and a complicated attracting set, shown in Fig. 2, appears. This complicated attractor exists for $\varepsilon_c^1 < \varepsilon < \varepsilon_c^2 \approx 3.205$. For larger values of ε the two-frequency torus is restored. Note that there are other regions of complicated behavior for large ε, however, here we do not want to discuss the whole space of parameters. To prove that the regime in Fig. 2 for $\varepsilon_c^1 < \varepsilon < \varepsilon_c^2$ is a strange non-chaotic attractor, we use the methods described in the Section 3.

4.1.1. Rational approximations

If we approximate the external frequency ω as $\omega_n = F_{n-1}/F_n$, we get the following mapping T_n:

$$x(t+1) = x(t) - B + \frac{A}{2\pi}\sin 2\pi x(t) + \varepsilon \sin[2\pi(t\omega_n + \theta_0)]. \qquad (10)$$

The external force has period F_n and depends on the initial phase θ_0. For each θ_0 there exists an attractor in (10), and the collection of these attractors for all $0 \le \theta_0 < 1$ gives a rational approximation of the quasiperiodically forced circle map. It is clear that it is sufficient to consider the F_nth iteration of the mapping (10) to obtain qualitative properties of the rational approximation. Furthermore, we can restrict θ_0 to the interval $[0, 1/F_n)$—this way we choose one point of the periodic orbit of θ. Since the map is invertible we are able to compute stable as well as unstable fixed points using forward and backward iterations.

For small ε the mapping $x(t) \to x(t+F_n)$ has a stable fixed point $x(t+F_n) = x(t)$ for all phases θ_0, if n is large enough. This situation changes in the region $\varepsilon_c^1 < \varepsilon < \varepsilon_c^2$. Here, depending on θ_0, there are different attractors. Considering only fixed points of the mapping T_n, there are three types of them: (1) $x(t+F_n) = x(t)$, (2) $x(t+F_n) = x(t) + 1$, (3) $x(t+F_n) = x(t) - 1$, with rotation numbers 0, $1/F_n$, and $-1/F_n$, correspondingly. These attractors are separated by "gaps"—regions of θ_0 where the F_nth iteration of (10) has no fixed points. The gaps are presumably filled by periodic (with periods larger than 1) and quasiperiodic orbits. A typical bifurcation diagram is shown in Fig. 3. The key observation is that this diagram is qualitatively the same for all approximations with odd large F_n. Thus, persistence of bifurcations in rational approximations ensures that the attractor is strange non-chaotic. The quantitative features of the bifurcation diagram change, however, with n. We found that these gaps disappear very rapidly, as can be seen in Fig. 4. Having four gaps (see Fig. 3), we average logarithms of their width and plot the logarithm of this average vs. the logarithm of the period (which is proportional to n). The points can be fitted by a line, what suggests that the widths decrease as exponent of the period of approximation. Thus, we can conjecture that a detailed structure of gaps becomes irrelevant as $n \to \infty$.

It is interesting to see how the bifurcation structure appears as the parameter ε is changed. For a particular rational approximation we demonstrate this in Fig. 5. As ε approaches the critical value, the distance between the sets of stable and unstable fixed points de-

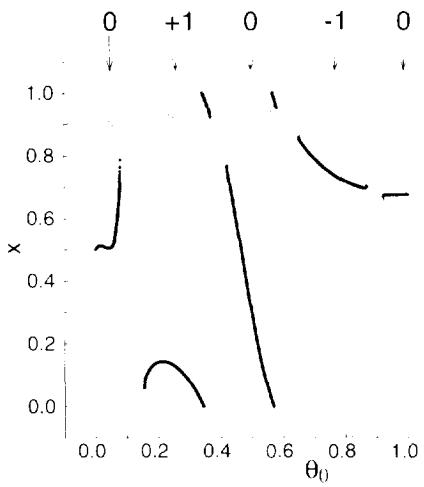

Fig. 3. Bifurcation diagram for the rational approximation $\omega_7 = 8/13$. The dots and the fat dots show unstable and stable fixed points of the type $x(t+13) = x(t) + G$ for different values of the phase shift θ_0. The regions with different G are marked by arrows.

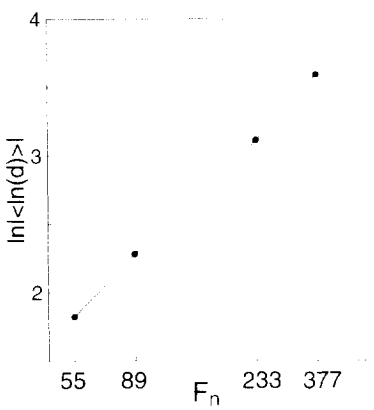

Fig. 4. Averaged width of gaps in the double logarithmic scale versus the period of approximation.

creases, and at $\varepsilon = \varepsilon_{cn}$ they touch at one point (as $n \to \infty$, the values of ε_{cn} converge to ε_c^1). For $\varepsilon > \varepsilon_{cn}$ a gap, and for larger ε a new fixed point $x(t+F_n) = x(t) \pm 1$ appear. Thus, one can say that the destruction of the two-torus to the strange non-chaotic attractor occurs through a bifurcation at which the stable and unstable two-frequency tori touch at a dense set of points. At each approximation the number of the points, at which the bifurcation diagrams touch, is proportional to F_n; it becomes an everywhere dense set of points when n goes to infinity.

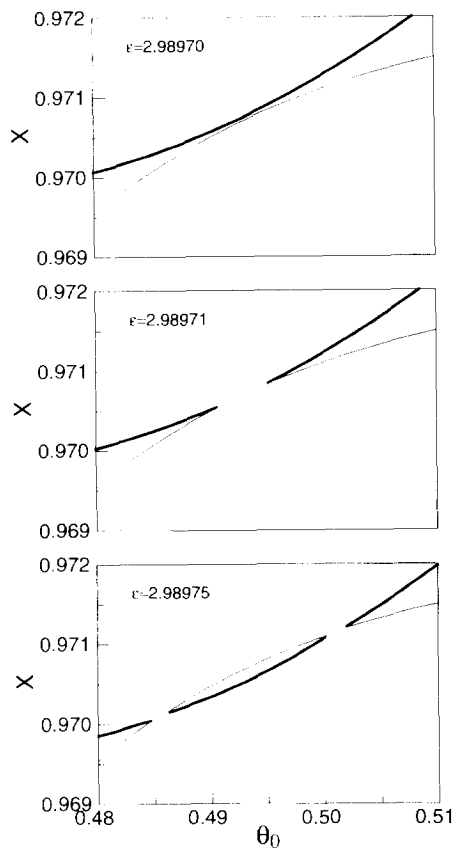

Fig. 5. Evolution of the bifurcation diagram with ε for the approximation $F_{11} = 89$. Dots: unstable fixed points, fat dots: stable fixed points. The central region on the bottom panel corresponds to the fixed points of the type $x(t+89) = x(t) - 1$.

A similar picture appears in the iteration of the quasiperiodically forced circle map (1), (2). Because this map is invertible too, one can iterate it forward and backward in time to obtain the stable and the unstable two-frequency tori. Near the critical parameter value ε_c^1 they come close to each other (Fig. 6) and at $\varepsilon = \varepsilon_c^1$ they touch in a dense set of points (touching at one point ensures touching at all its images which are dense on the interval $0 \le \theta < 1$). A similar transition has been observed in [8] for a forced logistic map.

There is another possible way for stable and unstable two-frequency tori to disappear, described in Ref. [18]. It occurs for small ε if the parameter B is changed. In this bifurcation the stable and the unstable tori do not touch at a dense set of points only, but at all

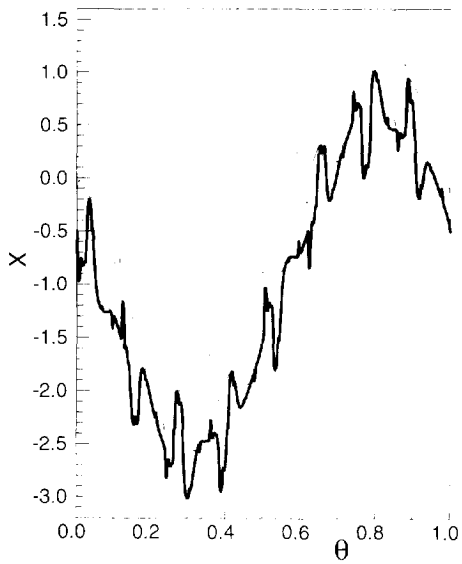

Fig. 6. Stable (fat dots) and unstable (dots) tori for $\varepsilon = 2.98$, just below the critical value ε_c^1.

points simultaneously. In a graph similar to Fig. 6 one can see that the distance between the tori decreases uniformly as the transition point is approached. Correspondingly, in rational approximations a range of values of the parameter B for which bifurcations in dependence on θ_0 are observed decreases with n. Such "annihilation" of stable and unstable tori does not give an SNA, but a three-frequency torus.

It is worth noting that the destruction of the stable torus and the appearance of the strange non-chaotic attractor resembles a well-known transition from torus to cantorus in Hamiltonian dynamical systems [23–27]. The difference is that in our case the gaps effectively disappear, and in each odd approximation the attractor consists of pieces having different rotation numbers. Therefore, it seems to be impossible to characterize the limiting set as a cantorus.

4.1.2. *Phase sensitivity and local Lyapunov exponents*

We calculate for the quasiperiodically forced circle map the phase sensitivity function $\Gamma(T)$ as described in Section 3.2. The results are presented in Fig. 7. For $\varepsilon < \varepsilon_c^1$ the phase sensitivity function saturates that means that the occurring attractor is non-strange. In

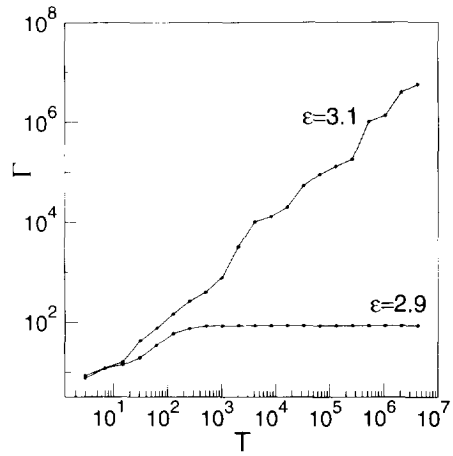

Fig. 7. The phase sensitivity function $\Gamma(T)$ for $B = 0$ and two values of ε, corresponding to a two-frequency torus ($\varepsilon = 2.9$) and to SNA ($\varepsilon = 3.1$).

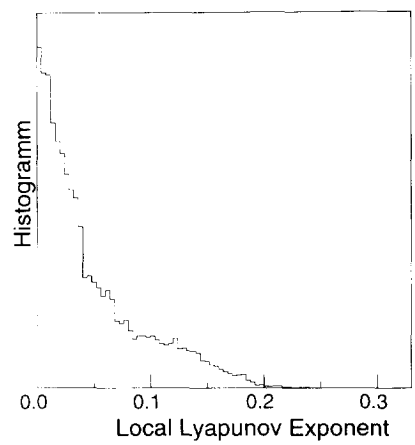

Fig. 8. Distribution of local Lyapunov exponents Λ_T for $T = 40$ on the SNA Fig. 2, obtained with 10^{10} iterations. Only the part of positive Λ is shown (the vertical scale is arbitrary).

contrast to that it grows in the region of SNA, giving a positive phase sensitivity exponent. Additionally, we calculate the distribution of local Lyapunov exponents. For the region of SNA $\varepsilon_c^1 < \varepsilon < \varepsilon_c^2$ we found that this distribution has a positive tail (Fig. 8) which corresponds to an interval of values of the local exponents Λ with $\Lambda > 0$. This gives another indication of the existence of SNA in the quasiperiodically forced circle map.

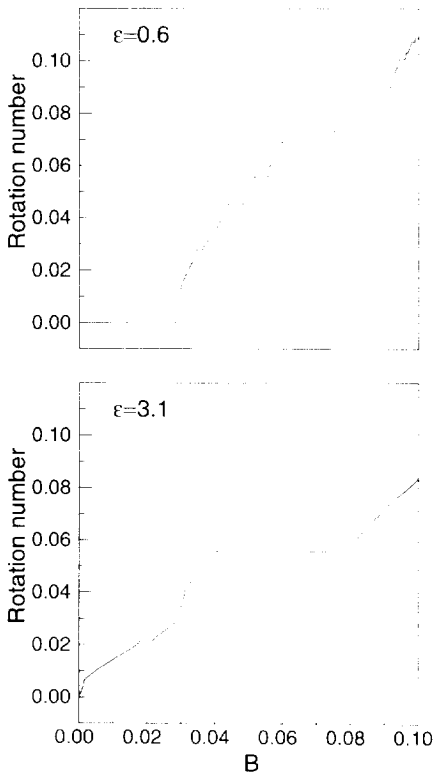

Fig. 9. Rotation number vs. B for two values of the amplitude of external force ε. For $\varepsilon = 3.1$, when the SNA is present for $B = 0$, only 6 steps are present (the resolution in B is 10^{-4}), while for $\varepsilon = 0.6$ 35 steps are observed with the same resolution.

4.2. *Disappearance of the devil's staircase*

The regime with SNA for $B = 0$ described in the previous section has zero rotation number, due to the symmetry $x \to -x$, $\theta \to 1/2 + \theta$. For $B \neq 0$ this symmetry is no more valid, and regimes with non-zero rotation numbers are possible. The dependence of the rotation number on B is of particular interest, because this is an experimentally observable quantity (e.g., for a driven Josephson junction this is the dependence of the voltage on the current, see [16,28]).

We report the dependence of the rotation number on B for two values of ε in Fig. 9. First, we would like to mention that the step with zero rotation number disappears when the SNA is present already for $B = 0$, i.e. in the region $\varepsilon_c^1 < \varepsilon < \varepsilon_c^2$. Indeed, if in the quasiperiodically forced circle map there is a stable two-frequency torus, it is separated from the unstable one, and they can collide only at a finite phase shift $B_c(\varepsilon)$. Therefore, the step with $\rho = 0$ has the finite width $2B_c(\varepsilon)$. In the regime with the SNA the stable and the unstable tori are already destroyed, and small variation of the parameter B produces persistent motion of the phase x.

This situation is similar to the chaotic case, which can appear for sufficiently large A and $B = \varepsilon = 0$. Unbounded chaotic motion produces diffusion of the phase x, and non-zero B gives asymmetry of hopping rates, ensuring the disappearance of the step with zero rotation number [28]. In the case of SNA (Fig. 2) we also observe diffusion of x, however, comparing to the chaotic case it is anomalously slow. It is rather difficult to investigate the diffusion of x quantitatively, because the dynamics of this variable has both diffusive and quasiperiodic components. To reduce the quasiperiodic component, we subtract from x an auxiliary quasiperiodic process z defined as

$$z(t+1) = z(t) + \varepsilon \sin(2\pi\theta(t)). \tag{11}$$

It is easy to check that $y = x - z$ obeys

$$y(t+1) = y(t) + B + \frac{A}{2\pi}\sin(2\pi x(t)). \tag{12}$$

A numerical study of the spreading of y shows that it grows as slow as the logarithm of time (Fig. 10). Such very low spreading means that all the orbits have the same rotation number, as it should be according to the theorem of Herman [29,18]. (For a chaotic system, where diffusion is normal, different trajectories can have different rotation numbers, although an average rotation number for the attractor is well defined.)

The rotation number can be also obtained from the rational approximations, discussed in Section 4.1.1 above. For fixed parameter values A, B, and ε we find for the approximation $\omega_n = F_{n-1}/F_n$ different stable solutions of the type $x(t+F_n) = x(t) + G_n(\theta_0)$, where the integer G_n depends in general on the initial phase θ_0. If the attractor is not strange, there are no bifurcations in dependence on the initial phase, and G_n does not depend on θ_0. In this case the nth approximation to the rotation number is $\rho_n = G_n/F_n$. If the attractor is strange, G_n does depend on θ_0 and to obtain the nth

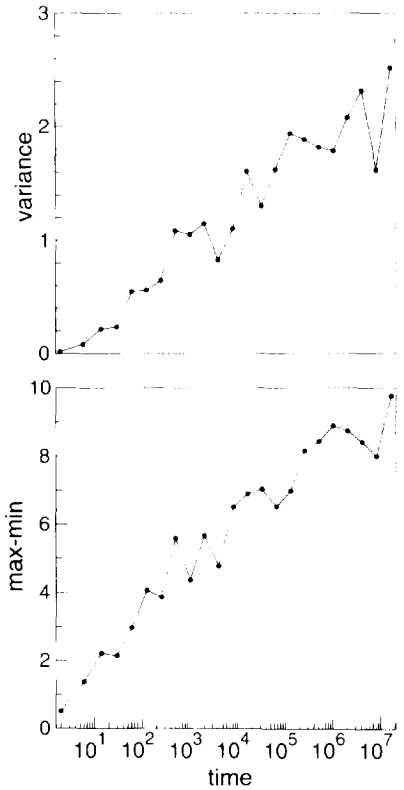

Fig. 10. Spreading of y in time. An ensemble of 1000 systems with different initial conditions has been run, and in this ensemble the variance (upper panel) and distance between the maximal and the minimal y were calculated. Both quantities grow roughly as a logarithm of time.

approximation to the rotation number we average over the initial phase:

$$\rho_n = \langle G_n(\theta_0)/F_n \rangle_{\theta_0}.$$

The rotation number obtained in this way is shown in Fig. 11. We see that the steps of the staircase are produced by the two-frequency regimes, while the strange non-chaotic attractor gives relatively smooth connection between these steps.

It should be emphasized that when the strange non-chaotic attractor is present, the staircase is no more complete (no more the devil's): in our numerical study we observe only a few steps. It appears that SNA is a relatively robust object: it exists in whole intervals of parameters. In these intervals there are no resonances (two-frequency tori with rotation numbers satisfying (4)) and the rotation number varies gradually. This

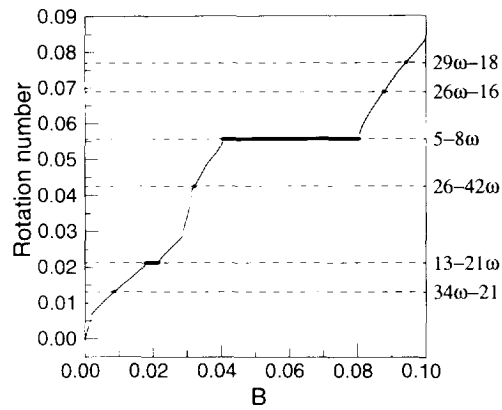

Fig. 11. Rotation number vs. B obtained from the rational approximations for $\varepsilon = 3.1$. The points, for which the approximations with periods 987 and 1597 have no bifurcations in θ_0 are marked with fat dots. The corresponding steps coincide with those in the bottom panel of Fig. 9, their rotation numbers are given.

"stability" of the SNAs make them different from the three-tori, which can be observed only on an open set of parameters, with resonances being everywhere dense.

This picture contradicts the conjecture of [2–5,12] that the SNA cannot correspond to a rotation number of the form (4). Already the appearance of SNA for $B = 0$ having zero rotation number contradicts this conjecture. Our results show that the two-frequency regimes have a rotation number of the form (4), while SNAs can have rotation numbers satisfying or not satisfying condition (4).

4.3. Lyapunov exponent

The Lyapunov exponent proves to be a good tool to distinguish between different regimes in the quasiperiodically forced circle map [2–5,12]. For the two-frequency torus and the SNA it is negative, and for the three-frequency torus it is zero. Thus, one can easily distinguish whether at the collision of the stable and the unstable two-frequency tori (which happens at finite B) the three-frequency torus or the SNA is created. Calculation of the Lyapunov exponent at the collision point $B_c(\varepsilon)$ allows us to find regions where the two-frequency torus disappears with the creation of the SNA (the Lyapunov exponent is negative) or with the appearance of the three-frequency motion (the Lya-

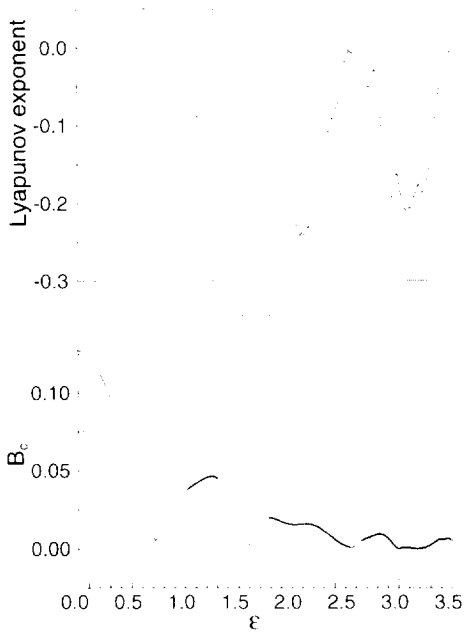

Fig. 12. The border of phase-locking interval region B_c and the Lyapunov exponent at this border. The regions with negative Lyapunov exponents (marked with fat dots) correspond to the transition to SNA. For $\varepsilon_c^1 < \varepsilon < \varepsilon_c^2$ the phase-locking interval shrinks: $B_c = 0$.

punov exponent is zero) (see Fig. 12). To these two transitions correspond two bifurcations of collision of the stable and the unstable two-tori (see Section 4.1 above): in one they touch in a dense set of points, in the other they touch at all points.

5. Conclusions

We have shown that in the quasiperiodically forced circle map the strange non-chaotic attractors can appear far from the transition to chaos. The existence of the SNA has been proved by different methods: via analysis of rational approximations and with calculation of phase sensitivity properties. The motion on the SNA is characterized by anomalously slow diffusion. We have argued that SNAs fill whole regions in the space of parameters, where the rotation number changes rather smoothly. In these regions there are no resonances, so the complete devil's staircase is destroyed when the SNA appears.

In this paper we have considered only the main phase-locking region, corresponding to the zero rotation number. The SNA can appear inside this region (for large amplitudes of external force) and at the boundary (for relatively smaller amplitudes). We expect that a qualitatively similar picture occurs in other phase-locking regions, where critical amplitudes of the quasiperiodic external force could be smaller. This will be the subject of a future study.

There are two characteristics of strange non-chaotic attractors that we do not discuss in this paper: dimensions and correlations. Dimensions of SNA were considered in [6], where it was suggested that they are multifractals with $D_0 = 2$ and $D_1 = 1$. It is, however, very difficult to verify these results numerically, because of huge computational time required. Indeed, the numerical results presented in [6] gave for different SNAs the values 1.8 and 1.95 for D_0, and 1.2 and 0.9 for D_1, using 10^9 points on attractors. It seems that basing oneself only on the numerics, it is hardly possible to characterize the fractal properties of the SNAs; one needs at least some examples where these can be obtained analytically.

Power spectra of SNA were considered in Refs. [2–5,12,11]. In Refs. [2–5,12] it was argued that the power spectrum of SNA is discrete, but very dense. In Ref. [11] an example of SNA was considered having a purely singular continuous spectrum. In the case of the forced circle map one can expect that the spectrum has both discrete and singular continuous components [30]. At present it is not clear, how practically to separate these components.

Finally, we discuss a possible experimental observation of the regimes with strange non-chaotic attractor in the system considered. It is known that a quasiperiodically forced Josephson junction and a quasiperiodically driven pendulum are described by a mapping similar to (1), (2) [3]. In the case of the Josephson junction the parameter B corresponds to the direct current through the junction, and the rotation number is the averaged voltage. Thus, the disappearance of the devil's staircase (Shapiro steps) in the voltage–current characteristics of the junction indicates the presence of the SNA. The most convincing fact could be the disappearance of the zero-voltage step, as in Fig. 9. A

work on extending the results of the present paper to the case of quasiperiodically forced Josephson junction is now in progress [31].

Acknowledgements

We thank P. Grassberger, S. Kuznetsov, V. Oseledec, A. Politi, U. Smilansky and M. Zaks for useful discussions and J. Stark for sending us the paper [18] prior to publication.

References

[1] C. Grebogi, E. Ott, S. Pelikan and J.A. Yorke, Physica D 13 (1984) 261.
[2] A. Bondeson, E. Ott and T.M. Antonsen, Phys. Rev. Lett. 55 (1985) 2103.
[3] F.J. Romeiras et al., Physica D 26 (1987) 277.
[4] F.J. Romeiras and E. Ott, Phys. Rev. A 35 (1987) 4404.
[5] M. Ding, C. Grebogi and E. Ott, Phys. Rev. A 39 (1989) 2593.
[6] M. Ding, C. Grebogi and E. Ott, Phys. Lett. A 137 (1989) 167.
[7] T. Kapitaniak, E. Ponce and J. Wojewoda, J. Phys. A 23 (1990) L383.
[8] J.F. Heagy and S.M. Hammel, Physica D 70 (1994) 140.
[9] A. Pikovsky and U. Feudel, Chaos 5 (1995) 253.
[10] S. Kuznetsov, A. Pikovsky and U. Feudel, Phys. Rev. E 51 (1995) R1629.
[11] A. Pikovsky and U. Feudel, J. Phys. A: Math. Gen. 27 (1994) 5209.
[12] M. Ding and J. Scott Kelso, Int. J. Bif. Chaos 4 (1994) 553.
[13] W.L. Ditto et al., Phys. Rev. Lett. 65 (1990) 533.
[14] T. Zhou, F. Moss and A. Bulsara, Phys. Rev. A 45 (1992) 5394.
[15] P. Bak, T. Bohr and M.H. Jensen, Phys. Scr. T 9 (1985) 50.
[16] M.H. Jensen, P. Bak and T. Bohr, Phys. Rev. A 30 (1984) 1960.
[17] O.E. Lanford, in: Recent Developments in Mathematical Physics, eds. H. Mitter and L. Pittner (Springer, Berlin, 1987) pp. 1–17.
[18] P.R. Chastell, P.A. Glendinning and J. Stark, Phys. Lett. A 200 (1995) 17.
[19] A.Ya. Khinchin, Continued Fractions (The University of Chicago, Chicago, 1949).
[20] G.H. Hardy and E.M. Wright, An Introduction to the Theory of Numbers (Clarendon, Oxford, 1979).
[21] A. Crisanti, G. Paladin and A. Vulpiani, Products of Random Matrices in Statistical Physics (Springer, Berlin, 1993).
[22] P. Grassberger, R. Badii and A. Politi, J. Stat. Phys. 51 (1988) 135.
[23] I. Percival, in: Nonlinear Dynamics and the Beam-Beam interaction, Vol. 57, eds. M. Month and J.C. Herra (AIP Conference Proceedings, 1979) pp. 1–17.
[24] S. Aubry and P.Y. LeDaeron, Physica D 8 (1983) 381.
[25] W. Li and P. Bak, Phys. Rev. Lett 57 (1986) 655.
[26] H.J. Schellnhuber, H. Urbschat and A. Block, Phys. Rev. A 33 (1986) 2856.
[27] H.J. Schellenhuber and H. Urbschat, Phys. Rev. A 38 (1988) 5888.
[28] A.S. Pikovsky, Zh. Tekhn. Fiz. 54 (1984) 381.
[29] M.R. Herman, Comment. Math. Helvetici 58 (1983) 453.
[30] H. Broer and F. Takens, Arch. Rat. Mech. Anal. 124 (1993) 13.
[31] U. Feudel, J. Kurths and A. Pikovsky, in preparation.